(49) Kobayashi, M.; Chen, J.; Chung, T.-C.; Moraes, F.; Heeger, A. J.; Wudl, F. *Synth. Met.* **1984**, *9*, 77–86.
(50) Hotta, S.; Hosaka, T.; Soga, M.; Shimotsuma, W. *Synth. Met.* **1984**, *9*, 381–387.
(51) Hotta, S.; Hosaka, T.; Soga, M.; Shimotsuma, W. *Synth. Met.* **1984/85**, *10*, 95–99.
(52) Neugebauer, N.; Neckel, A.; Brinderkoropic, N. In *Electronic Properties of Polymers and Related Compounds*; Springer-Verlag: Berlin, 1985; p 227.
(53) Brown, C. E.; Khoury, I.; Bezoari, M. D.; Kovacic, P. *J. Polym. Sci., Polym. Chem. Ed.* **1982**, *20*, 1697–1707.
(54) Clarke, T. C.; Scott, J. C.; Street, G. B. *IBM J. Res. Dev.* **1983**, *27*, 313–320.
(55) Devreux, F.; Bidan, G.; Syed, A. A.; Tsitavis, C. *J. Phys.* **1985**, *46*, 1595–1601.
(56) Hotta, S.; Hosaka, T.; Shimotsuma, W. *J. Chem. Phys.* **1984**, *80*, 954–956.
(57) Osterholm, J.-E.; Sunila, P.; Hjertberg, T. *Synth. Met.* **1987**, *18*, 169–176.
(58) Hotta, S.; Hosaka, T.; Soga, M.; Shimotsuma, W.; Taketani, M.; Kohiati, S. *J. Chem. Soc. Jpn., Chem. Ind. Chem.* **1986**, *3*, 365–372.
(59) Roncali, J.; Yassar, A.; Garnier, F. *J. Chem. Soc., Chem. Commun.* **1988**, *9*, 581–582.
(60) Elsenbaumer, R. L.; Jen, K. Y.; Oboodi, R. *Synth. Met.* **1986**, *15*, 169.
(61) Basescu, N. Ph.D. Thesis, University of California, Santa Barbara, 1988; p 108.
(62) Curtis, R. F.; Phillips, G. T. *Tetrahedron* **1967**, *23*, 4419–4424.
(63) Krische, B., private communication.
(64) Nowak, M. J.; Rughooputh, S. D. D. V.; Hotta, S.; Heeger, A. J. *Macromolecules* **1987**, *20*, 965–968.
(65) Bradley, D. D. C.; Friend, R. H.; Lindenberger, H.; Roth, S. *Polymer* **1986**, *27*, 1709.
(66) Tourrillon, G.; Garnier, F. *J. Electroanal. Chem.* **1982**, *135*, 173–178.
(67) Bohlmann, F.; Zdero, C. *Chem. Ber.* **1976**, *109*, 901–905.
(68) Takahashi, K.; Sone, C.; Fujieda, K. *J. Phys. Chem.* **1970**, *74*, 2765.
(69) Yesinowski, J. P.; Eckert, H.; Sandman, D. J.; Velasquez, C. S. In *Crystallographically Ordered Polymers*; Sandman, C. J., Ed.; ACS Symposium Series 337; American Chemical Society: Washington, DC, 1987; p 233.
(70) Hotta, S.; Rughooputh, S. D. D. V.; Heeger, A. J.; Wudl, F. *Macromolecules* **1987**, *20*, 212.
(71) Cazes, J. *J. Chem. Ed.* **1966**, *43*, A567–A582; *J. Chem. Ed.* **1966**, *43*, A625–A642.
(72) Sperling, L. H. *Introduction to Physical Polymer Science*; Wiley: New York, 1986; p 85.
(73) A referee asked for speculation regarding interpretation of this unusual result. The balance between intermolecular and intramolecular interactions that are responsible for the observation of high conductivities in doped conjugated polymers is still a matter of much controversy. No clean experimental results exist that establish a minimum conjugation length associated with high conductivity. In the poly(3,3′-dihexyl-2,2′-bithiophene) case, the conjugation length may, in fact be large but the intramolecular π overlap is diminished by a decrease in coplanarity of the polythiophene backbone and electronic transport may not be as sensitive to p_z–p_z π overlap as intuitively expected. Alternatively, in the poly(3,3′-dihexyl-2,2′-bithiophene) case intermolecular interactions may be enhanced relative to the predominantly head-to-tail poly(3-hexylthiophene) but intramolecular delocalization is inhibited, resulting in essentially no change in transport properties between these two regioisomeric polymers.
(74) Perrin, D. D.; Armarego, W. L. F.; Perrin, D. R. *Purification of Laboratory Chemicals*, 2nd ed.; Pergamon Press: Oxford, 1987.
(75) Gordon, A. J.; Ford, R. A. *The Chemist's Companion*; John Wiley & Sons: New York, 1972.
(76) Hotta, S. *Synth. Met.* **1987**, *22*, 103.

Registry No. **2**, 1693-86-3; **2** (homopolymer), 104934-50-1; **3**, 16494-40-9; **4**, 124561-55-3; **5**, 67984-20-7; **5** (homopolymer), 99836-43-8; **6**, 124535-72-4; **6** (homopolymer), 124535-74-6; iodine, 7553-56-2.

Junction Point Motion from ^{31}P NMR Line Shapes and Relaxation Times in Poly(propylene glycol)/Urethane Networks

L. Charles Dickinson,* J. C. W. Chien, and W. J. MacKnight

Department of Polymer Science and Engineering, University of Massachusetts, Amherst, Massachusetts 01003. *Received May 8, 1989; Revised Manuscript Received August 2, 1989*

ABSTRACT: ^{31}P NMR line shapes and spin–lattice relaxation times in the lab (T_1^P) and rotating ($T_{1\rho}^P$) frames have been measured over a wide range of temperatures for a series of network polymers with molecular weight between cross-links (M_c) ranging from 400 to 3000. The networks are formed from α,ω-dihydroxypoly(propylene glycol) and tris(4-isocyanatophenyl)thiophosphate. The line shapes are interpreted in terms of a diffusional motion model; the fit is reasonably good for short correlation times. The discrepancy between calculated and observed minimum relaxation times indicates the inadequacy of an isotropic motional model especially for lower M_c samples. Some computation of factors to correct for the nonisotropic motional case are included. Comparison with previous ^{13}C relaxation data shows that the ^{31}P motional frequency lags the segmental motion by a factor of 3 and 5 for the M_c 1000 and M_c 3000 cases, respectively. Correlation times obtained from the line-shape fitting and from the relaxation times do not agree; the former is about 3 times longer. This discrepancy may be attributed to the inadequacy of the relaxation model of isotropic averaging of the chemical shift anisotropy or to the over-simple motional model of the line-shape fitting, or both.

Introduction

The improvements in spectroscopic techniques and their use in combination are making possible the understanding of macroscopic phenomena of polymeric materials on a detailed molecular level. For instance, the dynamic mechanical modulus temperature dependence in polycarbonates has been analyzed in terms of a distribution of correlation times determined from nuclear magnetic resonance[1] with motion including libration and 180° aromatic ring flips.[2]

For poly(dimethylsiloxane) network systems neutron

0024-9297/90/2223-1279$02.50/0

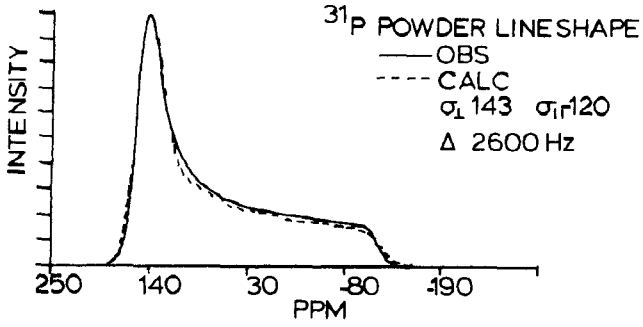

Figure 1. ^{31}P NMR spectrum of M_c 425 network at 173 K (—) shown with simulated powder spectrum line shape (- - -) computed for $\sigma_\perp$ = 143 ppm, $\sigma_\parallel$ = -120 ppm, line width = 2600 Hz.

scattering data showed that the individual chains do not distort affinely; this has resulted in some refinement of elasticity theory.[3] Fluorescence depolarization[4] and nuclear magnetic resonance[5,6] have been used to quantitatively measure the segmental motion in equilibrium, swollen, or stretched states of networks.

Our recent work[7] has focused on the role of the cross-link in molecular dynamics of well-defined networks prepared from near-monodisperse poly(propylene glycol) chains and a high-purity trifunctional isocyanate cross-linking agent. There is a large earlier body of literature on the NMR of networks,[8-13] but none explicitly treat the cross-link point mobility separate from the mobility or orientation of the connecting segments. This paper gives a detailed analysis of ^{31}P NMR line shapes and relaxation times of the junction points in these model networks as a function of temperature and molecular weight between cross-links, M_c.

Experimental Section

The exact preparation of these networks has been previously described.[7] Networks were prepared in bulk from near-monodisperse α,ω-dihydroxypoly(propylene glycol) of nominal molecular weights 425, 1000, 2000, or 3000. These samples are designated, respectively, M_c 0.4K, M_c 1K, M_c 2K, M_c 3K. Urethane linkages were formed by reacting in precise stoichiometry one of the prepolymers with tris(4-isocyanatophenyl)thiophosphate in bulk at 80 °C. Samples were stored at 5 °C in a vacuum desiccator to retard hydrolysis of the phosphate bonds, and spectra were obtained while spinning with dry nitrogen. The absence of change in the ^{13}C NMR relaxation times at room temperature was used as an index of stability. Samples showing a greater than 15% change were rejected, but with the above precautions samples were stable for some months.

NMR measurements were made on an IBM Instruments AF200 spectrometer with an IBM Solids Accessory and Doty Scientific CP-MAS multinuclear variable-temperature probe. For relaxation measurements samples were spun at about 5 kHz. Spinning speeds were lower at lower temperature down to about 2 kHz at -100 °C. A number of samples were run to compare spinning versus nonspinning relaxation times; no significant differences were found. The spin lock field for rotating frame measurements was 50 kHz; thus, both ^{31}P and ^{1}H 90° pulses were 5.0 μs. Cross polarization was used to obtain spectra at low temperature or for low M_c samples at higher temperatures. "Direct" polarization (a simple 90° ^{31}P pulse with ^{1}H decoupling during acquisition) was used if cross polarization was inefficient. The basic pulse sequences for obtaining spectra, T_1 and $T_{1\rho}$, are described in our previous papers.[6,7] High-power proton decoupling was used in most cases but resulted in no change in line shape except for the most rigid cases of low temperature and low M_c.

Some of our previously published spectra of these networks were subject to a distortion.[6] The clearest sympton of the distortion takes the form of a hump at the $\sigma_\parallel$ position of the powder pattern. This distortion could be eliminated in most cases by acquiring the FID as an echo as shown in Figure 1. The

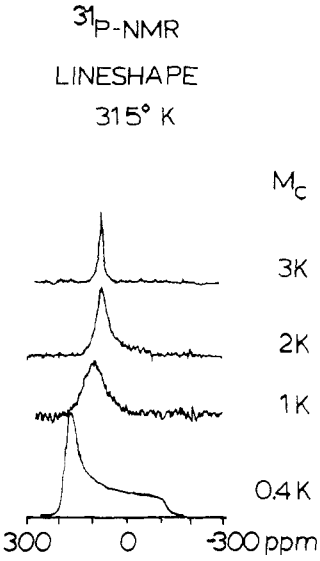

Figure 2. Line shape of ^{31}P NMR spectra at 315 K for a series of networks with M_c = 425, 1000, 2000, and 3000 as marked.

observed line shape from the transform of the echo matches well the shape calculated for the rigid lattice powder pattern and yields axial tensor components of $\sigma_\parallel$ = -120 ppm and $\sigma_\perp$ = 143 ppm referenced to solid $CaHPO_4$ as zero. This agreement of observed and calculated powder patterns shows that the distortion has been eliminated. This criterion is not so simple for the spectra from less rigid samples, and there may be a small amount of residual distortion. Fortunately these line shapes are much narrower so the problem is proportionately smaller. Subsequent to acquiring the data included in this paper we learned of an elegant detailed analysis and method of reduction of this phasing problem.[14]

Because there is some possibility of hydrogen bonding between carbonyl and amide groups of the urethanes, which could cause aggregation in these network systems, we performed a one-dimensional exchange ^{31}P-^{31}P experiment adapting the pulse sequences of Conner et al.[15] Even though there is only one type of phosphorus present, one can null any part of the chemical shift anisotropy (CSA) powder spectrum, say the part near $\sigma_\parallel$, and examine that region over the long T_1^P period of up to 25 s for any return of intensity by exchange with spins contributing to other parts of the spectrum. No evidence of such phosphorus exchange was found even in the M_c 0.4K sample, which has the smallest ^{31}P-^{31}P distance. This result shows that the inter-^{31}P radii are greater than 1.5 nm.

Line-shape computation was performed on the University of Massachusetts VAX Cluster using programs based on the diffusion step model of Sillescu.[16] The programs used were from the laboratory of Professors A. Jones and P. Inglefield at Clark University. Observed line shapes were manually digitized for comparison with computed line shapes.

Results

Line-Shape Analysis. ^{31}P NMR line shapes at 315 K with varying M_c in these poly(propylene glycol)/urethane networks with phosphorus as the junction point are shown in Figure 2. The observed shape for the M_c 0.4K sample is that for an axially symmetric chemical shift tensor and implies reorientation of the phosphorus–sulfur axis is occurring at a frequency less than the spread of the line shape which is 22 kHz. As M_c increases, the line shape changes dramatically to a broad line with its maximum shifting to higher field. For M_c 3K the very narrow line is positioned at the isotropically averaged chemical shift, σ_{iso}. A very similar change in line shape is seen for these same networks as a function of temperature in Figure 1 of ref 7. Because of the above-mentioned phasing problem, a new set of spectra were obtained on a fresh sample of M_c 1K using simple spin

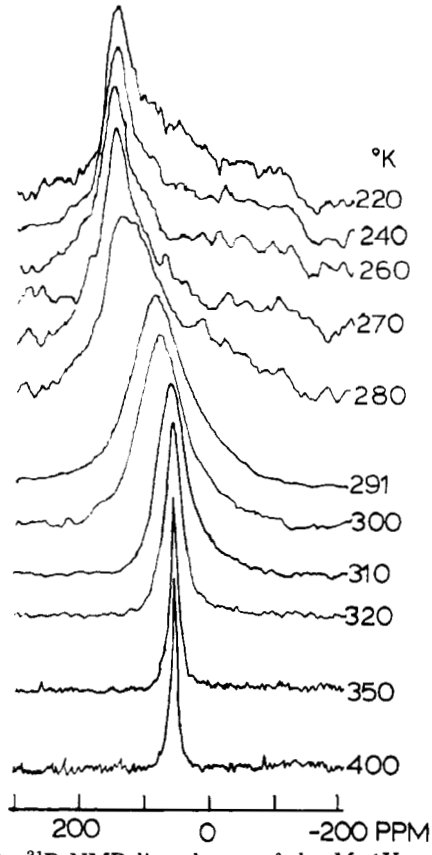

Figure 3. ^{31}P NMR line shapes of the M_c 1K network over the range of temperatures from 220 to 400 K as marked.

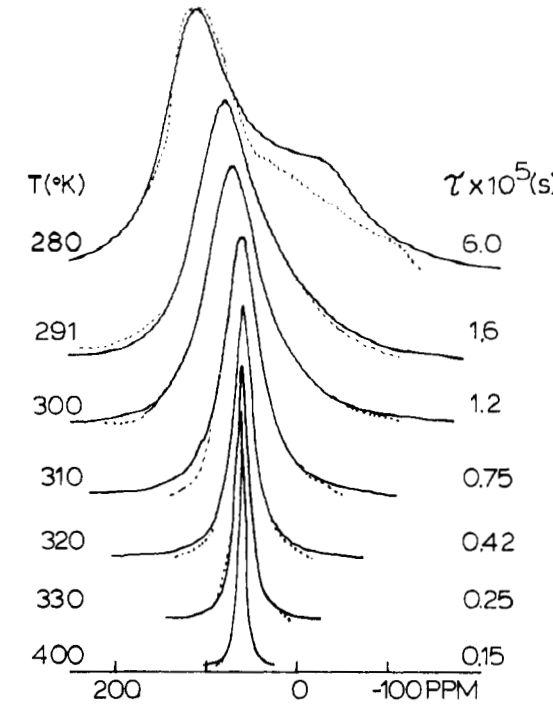

Figure 4. Comparison of observed ^{31}P NMR line shapes with those calculated for the diffusion model described in the text for the diffusion rates indicated on Figure 5.

echos for the broader line shapes (Figure 3). These line shapes, which are intermediate between axially symmetric and narrow liquidlike, contain information about the molecular motion in the networks which can be extracted by modeling.

The model for molecular dynamics used in this work was derived entirely from Sillescu[16] and requires formation of a N-dimensional matrix **A** where N is the number of magnetic sites across the spectrum. The elements of **A** are determined by the rate of the diffusion stepping between sites i and j, π_{ij}, and site frequencies, ω^i. The problem of determining the line shape is the same as diagonalizing **A**

$$S^{-1}\mathbf{A}S = \Lambda \tag{1}$$

which gives the transformation matrix elements S_{ij} and the eigenvalues Λ_{ij}. The line shape is then the sum of probability terms as described by Sillescu.[16] For this diffusion model one can choose the step spacing and solid angle for motion between sites across the axial spectrum with $x_i = \cos\theta_1$, the direction cosine of the ith site. With $\Delta = (x_{min} - x_{max})/N$, the only nonzero off-diagonal elements are adjacent to the diagonal

$$A_{ij} = \pi_{i,i+1} = (6\tau)^{-1}(x_i/\Delta)^2 \tag{2}$$

with $A_{ij} = A_{ji}$. The diagonal elements are

$$A_{ii} = -A_{i,i+1} - A_{i,i-1} + i\omega_i \tag{3}$$

T_2 broadening is convoluted into the calculated intensities. The program evaluates the **A** matrix, diagonalizes it, and determines the eigenvalues and the summation over angles in the same way as Sillescu.[16] A limit of the present computation is that diffusion over less than a complete octant results in averaging about only a limited set of orientations of the CSA tensor. For these unoriented materials all orientations of the CSA tensor must be considered.

We have calculated the line shape for the case of fully isotropic diffusion, all orientational elements being equally weighted so that the range of Θ is 0°–90°, and the only variable is the number of sites, N. The diffusion increment size is then $90/(N-1)$ deg, and τ is the only adjustable parameter for fitting the observed line shape. A line broadening of 111 Hz is included.

We are currently writing an appropriate program to include diffusional reorientation over less than the full 90° anisotropy and that includes libration about all possible orientations. The expected result is broader lines for the same correlation time so that a given observed line shape will require shorter correlation times for fitting. It is also expected that there will be more intensity in the wings of the calculated diffusion line shape than for the line shapes calculated here for diffusion through a full octant. Thus a shift to shorter τ is expected for the diffusion model with all orientations considered. This issue is an important one in view of the inference from the relaxation data below that the reorientation of the chemical shift tensor is undergoing libration at about a half-angle of 40°.

Computed line shapes for the M_c 1K sample spectra are shown in Figure 4 along with the observed spectra. The agreement is quite satisfactory over the range $\tau = 10^{-6}$ (400 K) to $\tau = 1.6 \times 10^{-5}$ (291 K). The fitting is best for the upper 80% of the line shape; the calculated shape has a wider base than the observed shape. A plot of these correlation times versus inverse temperature appears as Figure 5. The results for M_c 3K yield a linear Arrhenius plot over a limited temperature range. The data of M_c 1K spans a wider range and is linear up to the temperature where T_1^P is a minimum. The higher temperature change of slope will be discussed in a later section.

Relaxation Time Analysis. Figures 6 and 7 show, respectively, spin–lattice relaxation of ^{31}P in the laboratory frame (T_1^P) and the rotating frame ($T_{1\rho}^P$) for M_c

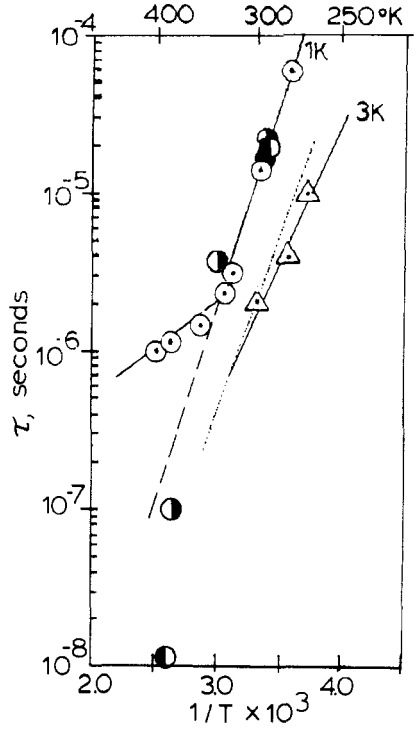

Figure 5. Log τ versus $1/T$ for correlation times determined from diffusion model line-shape fitting for 1.8-deg steps for M_c 3K (▲) and M_c 1K (⊙). For the M_c 1K case fitting was also done with 0.9- (●), 4.5- (◑), and 9-deg (◐) steps. The dotted line is the correlation time dependence determined from relaxation times for M_c 1K and is transcribed from Figure 9.

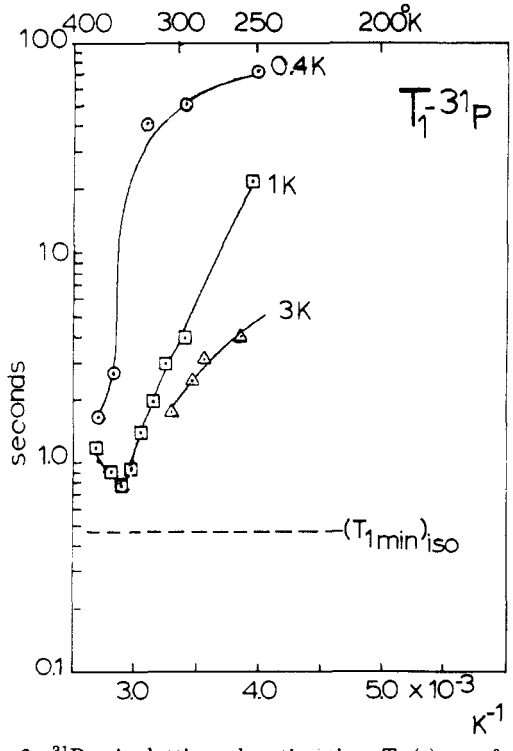

Figure 6. ^{31}P spin–lattice relaxation time T_1 (s) as a function of $1/T$ (K^{-1}) for M_c 425 (⊙), M_c 1000 (⊡), and M_c 3000 (▲).

0.4K, M_c 1K, and M_c 3K samples over a wide range of temperature. The data for the M_c 2K are very close to those of the M_c 1K and are omitted for clarity. The T_1^P data show a clear minimum in the M_c 1K, case although the partial curves in Figure 7 suggest the minimum would shift to lower temperature with higher molecular weight. Minima in $T_{1\rho}$ are observed for all three samples. The

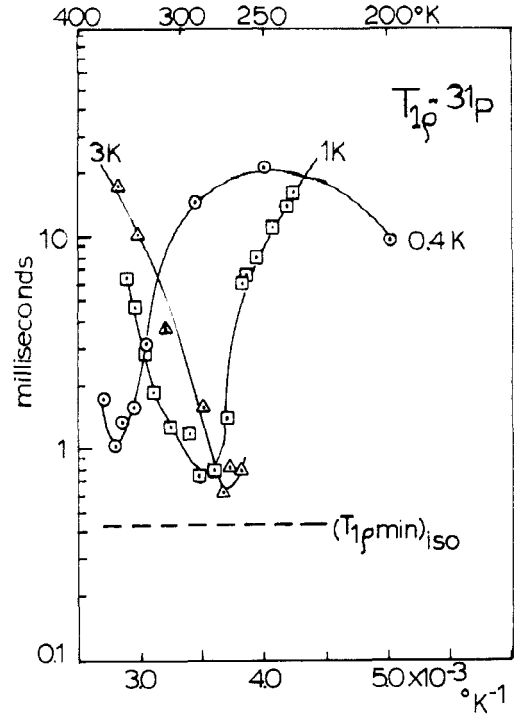

Figure 7. ^{31}P spin–lattice relaxation times in the rotating frame $T_{1\rho}$ (ms) as a function of $1/T$ (K^{-1}) for M_c 425 (⊙), M_c 1000 (⊡), and M_c 3000 (▲).

values of both $T_{1\rho,\min}$ and the temperature at which the minimum occurs decrease with increasing M_c.

Relaxation times and line shapes are both the result of specific molecular motions. While there are a number of examples of computation of line shape with motional theories especially for ^{2}H line shapes, there are few instances of careful analysis of both relaxation times and line shapes. Jones and co-workers[1] were able to construct a motional model that generates a reasonably consistent set of relaxation times and line shapes in polycarbonates. The case of ^{31}P NMR line shape and relaxation times for these networks is somewhat less favorable than the polycarbonate case for several reasons. For the axially symmetric ^{31}P tensor the motion rotating about the z axis is not detected, whereas the asymmetric ^{13}C CSA tensor in polycarbonates makes for line-shape sensitivity to motions in all directions. In addition, the polycarbonate motions are subtle with averaging of selected components of the CSA before the complete line-shape collapse. Most of our ^{31}P CSA data involves collapse to a featureless line of varying width at σ_{iso}.

The electronic environment of the phosphorus nuclei in these networks is axially symmetric as shown by the low temperature or low M_c spectra such as Figure 1. The dominant mechanism of relaxation in these networks is by reorientation of the CSA. Our observation that proton decoupling does little to the line shape in these networks eliminates heteronuclear dipole–dipole (IS) relaxation as a significant mechanism of relaxation for the ^{31}P nuclei, and there are not other reasonable contending mechanisms. The unimportance of the IS mechanism is also expected as there are no nearby or bonded protons to the phosphorus atom. As noted below isotropic CSA theory predicts relaxation times too short compared to the observed minima; an additional mechanism such as IS would shorten the predicted time even more and thus increase the discrepancy. All subsequent analysis of relaxation times in this paper is based exclusively on the CSA mechanism.

The theory of isotropic CSA relaxation has been developed along the basic formalism originated by Bloembergen, Purcell, and Pound[17] for dipolar relaxation. Parallel equivalent equations for CSA reorientation relaxation have been developed by a number of authors[18-20] to yield the following equations, which we use in Mehring's[19] format

$$(T_1^{-1})_{CSA} = \gamma^2 B_0^2 \{j_{11}(\omega_I) + j_{21}(\omega_I)\} \quad (4)$$

$$(T_{1\rho}^{-1})_{CSA} = \gamma^2 B_0^2 \{j_{00}(\omega_e)/3 + j_{11}(\omega_I)/2 + 2j_{20}(\omega_e)/3 + j_{21}(\omega_I)/2\} \quad (5)$$

where the $j_{kq}(\omega)$ are the spectral density functions containing the symmetry and averaged fluctuations of the magnetic interactions, $\omega_I = \gamma B_0$, $\omega_e = \{(\gamma B_1)^2 + (\omega - \omega_I)^2\}^{1/2}$, γ is the gyromagnetic ratio of the nucleus measured, B_0 is the dc magnetic field; B_1 is the spin lock field and ω is the observing frequency. The spectral densities, $j_{kq}(\omega)$, are the Fourier transforms of the fluctuations in time

$$j_{kq}(\omega) = \mathrm{Re} \sum \mathrm{d}t\, (-1)q\, \langle \partial A_{kq}(t=0)\, \partial A_{k,-q}(t) \rangle e^{-i\omega t} \quad (6)$$

where the A_{kq} are components for the CSA interaction in terms of irreducible spherical tensors. For the isotropic case assuming no fluctuations of the chemical shift tensor on an NMR time scale, i.e., no molecular changes, $\partial A_{00} = 0$. For the axially symmetric case of these ^{31}P sites the antisymmetric components of the chemical shift tensor are negligible, $\partial A_{1q} = 0$, and only the fluctuations of the traceless symmetric part of the chemical shift, ∂A_{2q}, contribute to the relaxation. It is important to realize that the A_{kq} values are evaluated in the laboratory fixed frame governed by the direction of B_0 and transformation from the molecular principal axis fixed frame to the lab frame is accomplished with Wigner rotation matraices, which are a convenient way of averaging as detailed by Spiess.[19] It is characteristic of the isotropic case that averaging of the A_{2q} orientational fluctuations greater than 90° for all orientations of B_0 results in

$$T_1^{-1} = (2/15)\gamma^2 B_0^2 (\sigma_\parallel - \sigma_\perp)^2 \tau/(1 + \omega_P^2 \tau^2) \quad (7)$$

where the full range of the anisotropy of the CS tensor contributes to the motionally induced magnetic fluctuations felt by the ^{31}P nuclei. For $T_{1\rho}$ the spectral density terms dependent on $\omega_P = 2\pi 80 \times 10^6$ rad s^{-1} will not contribute significantly in comparison to the densities at the spin lock frequency, $\omega_e = 2\pi 50 \times 10^3$ rad s^{-1}; the former can be dropped, leaving only the $j_{20}(\omega)$ term. For isotropic motion all j_{2q} values will average to the same value,[19] yielding

$$T_{1\rho}^{-1} = (4/45)\gamma^2 B_0^2 (\sigma_\parallel - \sigma_\perp)^2 \tau/(1 + \omega_e^2 \tau^2) \quad (8)$$

Equations 7 and 8 predict the minima (at which $\omega\tau = 1$) for T_1 (0.45 s) and $T_{1\rho}$ (0.43 ms) shown in Figures 6 and 7, respectively. In both cases the observed values for M_c 1K are about a factor of 2 longer than those predicted on the basis of the isotropic model. This discrepancy probably arises because the P–S axis is not isotropically reorienting. Qualitatively and intuitively, if the motion of the molecular fixed axis system does not sweep through a full 90°, then the factor $(\sigma_\parallel + \sigma_\perp)^2$ in eqs 7 and 8 will be too large and thus the predicted relaxation times will be too small. If this factor can be reduced by some appropriate averaging process, then the calculated T_1 or $T_{1\rho}$ will better agree with the observed values. This incomplete averaging of the anisotropy is consistent with the NMR spectra. In the case of M_c 1K the line position has not reached σ_{iso} at the temperature of the $T_{1\rho}$ minimum (285 K). However, at the temperature of the T_1 minimum (345 K) the spectral position has reached that of the liquid line. It is also interesting that with increased M_c the $T_{1\rho}$ minimum approaches a lower value as shown in Figure 7. This shows a progressive approach to more isotropic motion with a lower degree of cross-linking.

Howarth[21] has treated the motional problem of libration, but for the case of IS relaxation. Because both CS and IS relaxation depend upon the same orientational spherical harmonics, the result is transferable to our case. A rigorous treatment of the problem of CS averaging $\langle \{\sigma(\theta,t) - \sigma(\theta',t+\tau)\}^2 \rangle$ where $\langle \theta - \theta' \rangle$ is less than 90° will be given as a separate paper.[22] While the symmetry of the reorientation for IS and CS is the same, it is not clear how the CS anisotropy prefactor in eqs 7 and 8 should be averaged for the case of limited reorientation. Howarth computes the IS relaxation functions for a model that restricts the reorientation of the internuclear C–H vector to a cone of half-angle θ, arriving at a result where the spectral densities are reduced by a multiplicative factor $(1 - A)$ where

$$A = \{(\cos\theta - \cos^3\theta)/2(1 - \cos\theta)\}^2 \quad (9)$$

The factor A has a range of [0,1]. This formalism has been applied to polymer segmental librations as distinct from Hall–Helfand segmental dynamics.[5] The observation that both T_1 and $T_{1\rho}$ minima are about a factor of 2 longer than the isotropic case prediction argues that the factor A in front of the spectral density functions is about the same at the minimum point for each relaxation time for each case. This would mean that the libration half-angle, θ, does not change significantly between 285 and 345 K but remains constant at about 40° or A = 0.5. This implies that the constraints on the spatial motion are not very temperature dependent so that increasing the temperature only increases the *frequency* of motion of the cross-link within those amplitude constraints.

Relationship between Segmental and Cross-Link Point Motions. The major design in studying these networks is the clarity of separately observing the dynamics of the cross-link point (^{31}P) and the dynamics of the connecting segments (^{13}C). Figure 8 shows the ^{31}P $T_{1\rho}$ data from this work plotted with the ^{13}C $T_{1\rho}$ data from our previous study.[7] Both curves are for identical M_c 1K samples. It is reasonable to compare the two relaxation curves because frequency and single-correlation time dependence of the spectral densities in the relaxation time expressions can be reduced to the same functions regardless of the differences in prefactors for the IS and CS relaxation mechanisms.[19] That is, CS and IS relaxation expressions will have the same $\tau/(1 + \omega^2\tau^2)$ factor. The absolute values of T_1 and $T_{1\rho}$ predicted for IS and CS will differ, but the shape of the log (relaxation time) versus $1/T$ plots should be the same. According to the data, clearly the minima are not reached at the same temperature, indicating differential mobility of the carbon segments and the phosphorus cross-link. These plots can be converted to log τ versus $1/T$ plots by assuming that the shape function above is correct although the absolute values are offset by some constant multiplier. Thus plotting the observed data as log $(T_{1\rho}/T_{1\rho,min})$ versus $1/T$ and comparing abscissas for equal ordinate values on a plot of log $\{\tau/[1 + (2\pi 50 \times 10^3)^2\tau^2]\}$ versus τ, one converts temperatures to τ's. This mapping of τ from temperature is plotted as log τ versus $1/T$ as shown in Figure 9. One can see that at a given temperature the correlation time for the carbon motion is shorter than that for the phosphorus motion by about a factor of 3. Thus

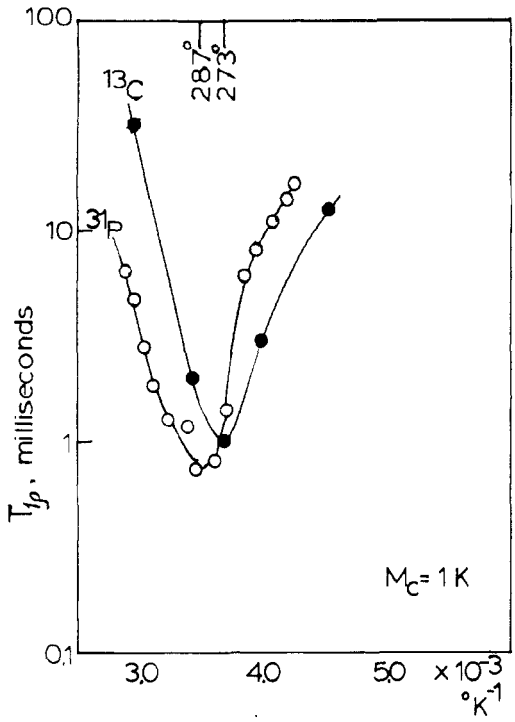

Figure 8. Comparison of ^{31}P (○) and ^{13}C (●) spin-lattice relaxation in the rotating frame $T_{1\rho}$ versus $1/T$ (K^{-1}) for M_c 1000 sample.

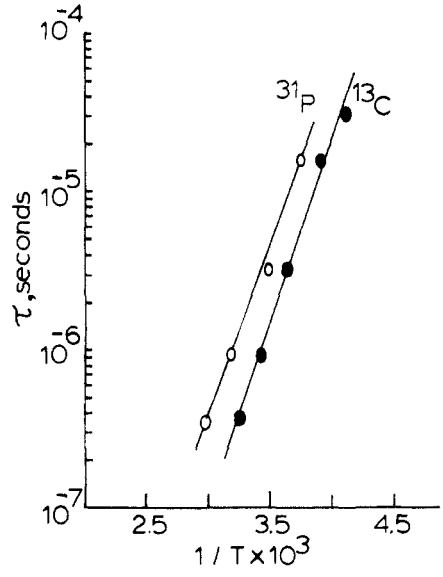

Figure 9. Plots of log τ versus $1/T$ (K) for the ^{31}P (○) and ^{13}C (●) data of Figure 8 for τ calculation based onn an isotropic relaxation model.

on this model the cross-link frequency lags the segmental frequency by about a factor of 3. The slopes of the plots are virtually identical, yielding on Arrhenius analysis an activation energy of 10.8 kcal. The equality of the ^{13}C and ^{31}P slopes indicates that the motions of each species may be coupled so that the segmental motion and cross-link motion differ by what may be called an entropy, which would be the intercept term at $1/T = 0$. Similar data analysis can be performed on the $T_{1\rho}$ data for the M_c 3K sample resulting in the same slope as for M_c 1K but with a factor of 5 separation in the τ values for the two nuclei. This indicates that in the longer chain networks the coupling is somewhat weaker, resulting in a larger lag in frequency between the cross-link motion and the chain motion. This lag factor is especially reliable because the difference is apparent at the minima of the ^{13}C and ^{31}P $T_{1\rho}$ data in Figure 8 at which the value of τ is most accurate. The origin of the lag may lie in an inherent property of cross-link points anchored by three chains or in the anchoring effect of the rather bulky cross-link molecule of these networks. The discrimination of these causes depends upon the extent to which the aromatic rings participate in the random chain statistics of the PPO chains, which can only be resolved by preparation of chains without the bulky cross-link.

Discussion

Cross-linked systems have been investigated by various techniques. Gronski et al.[12] examined poly(1,4-butadiene) networks with deuteration either along the whole chain or only near the cross-link point. They concluded that deformation was inhomogeneous with "excess orientation near network junctions". Our results showed a difference in dynamics of the cross-link point, and the bulk exists even for the undeformed networks. Monnerie et al.[23] attached fluorescent anthracene probes to bulk polyisoprene to quantify reorientational mobility. Some recent neutron spin-echo (NSE) studies by Oeser et al.[24] studied the spatial fluctuations of cross-link points in poly(dimethylsiloxane) (PDMS) and found that the "time scale of motion for the crosslinks is comparable to the time scale of segmental diffusion within the chains attached to the junctions". The differences with our work may reflect the extreme flexibility of the PDMS backbone and/or the anchoring effect of our bulky cross-linking moiety.

It is of interest to compare the correlation times obtained independently from ^{31}P relaxation analysis (Figure 9) to those obtained from line-shape analysis in the first part of this paper (Figure 5). In all cases the correlation times obtained from the line-shape analysis are longer, and for M_c 1K the discrepancy is a factor of 6; for M_c 3K it is about 3. Given the above-discussed limitations of the line-shape and relaxation analyses, this discrepancy between the methods of determining τ is not surprising, but the direction of the discrepancy suggests that some shorter τ values are being missed by the line-shape analysis. The discrepancy between the slopes of the log τ versus $1/T$ plots for the two techniques in the higher temperature regime also suggests that a temperature-dependent process such as increase in libration angle, ignored in the line-shape model used, may be important.

The above analysis is based on correlation times derived from $T_{1\rho}^P$. In the analysis of T_1^P the minimum based on the isotropic relaxation model will occur at $\tau = 2 \times 10^{-9}$ s, which is at 345 K ($1/T = 2.90 \times 10^{-3}$ K^{-1}) for M_c 1K. This point is 2 orders of magnitude below the ^{31}P line derived from $T_{1\rho}$ data in Figure 9! Plots like those of Figure 9 but based on T_1^P data have a slope of 10 kcal. The line-shape and $T_{1\rho}$ analyses for correlation times are thus widely discrepant from the T_1 analysis. One must bear in mind that the most reliable points in this analysis are those correlation times derived from the minima where one is reasonably certain that $\tau = \omega^{-1}$. The procedure used above for conversion of relaxation times to τ values over ranges beyond the minimum points is the simplest approximation for converting temperatures to τ values. If the two minima for T_1^P and $T_{1\rho}^P$ are taken as the only reliable points the activation energy of τ versus T^{-1} is 13.4 kcal/mol, a not unreasonable value for moving a bulky cross-link environment such as these networks have. The discrepancy will probably clear up when better interpretations are devised for the nonisotropic CSA case and a more versatile diffusion step line-shape model is implemented.

The temperature dependence of correlation times determined from the line-shape analysis as presented in Figure 5 shows an interesting break. In the low-temperature region of 250–320 K the plot is reasonably linear for the diffusion step arbitrarily held constant to 1.8 deg. Several points calculated for larger diffusion steps do not deviate much from the 1.8-deg step points. This indicates that for low temperature where the line shape is broad, the computed shape is relatively insensitive to step size. These line-shape-determined τ's can be compared with those determined from the relaxation times, which have been drawn onto Figure 5 as a dotted line. Clearly the τ values from line shapes are a factor of 3–6 longer than those from relaxation times over the low-temperature range. Under the limitations described above for both the line-shape and the relaxation models this discrepancy is not surprising. The apparent change of slope near 330 K is quite interesting. It is well above T_g and the $T_{1\rho}$ minimum for the M_c 1K material. The temperature 330 K is near the minimum for T_1 where the line shape reaches the isotropic position. As discussed above this isotropic position implies that the P–S axis is reorienting at a frequency higher than the CSA, but the angular displacement must be greater than 90°. If we make the simplest assumption that there is one mechanism of relaxation and line shape averaging over the entire temperature range, then the change of slope at 330 K probably means that above that temperature the diffusion steps become larger. Thus by increasing the step size one could linearize the line-shape-calculated times as a function of inverse temperature. Unfortunately, the relaxation time plot of Figure 9 extends only to a little above 330 K so that the linearity over the temperature range cannot be corroborated.

One must bear in mind that the determination of τ from the short τ line shapes is not unique. This fact is indicated in Figure 5 where values of τ corresponding to diffusion jumps of 0.9, 1.8, 4.5, and 9 deg are shown. Another limitation of this calculation is of course that the diffusion model breaks down as the steps get larger. A similar line-shape analysis with a 1.8-deg step was performed on the M_c 3K sample, yielding the points shown in Figure 5. In this case the error is somewhat larger because of the lower signal to noise ratio on the observed spectra and the narrow temperature range of observable spectra. It appears that the cross-link points in this higher M_c network are moving 1 order of magnitude faster than those in the M_c 1K network at a given temperature.

The fitting discrepancy at 280 K in Figure 4 suggests a breakdown of the diffusion model. An alternative is the jump model with its larger changes of orientation: this is physically unreasonable as the jumps have to be large and are thus less likely at the lower end of our temperature range. Although we made some computations based on the jump model,[25] in the range of τ required to get the width of the observed line shape even larger deviations than with the diffusion model were observed, particularly in the form of large humps presumably due to the limitations on the number of sites, up to 6, considered. For precise line-shape fitting in the lower temperature regime a model combining both diffusional and jump motion may be required.

Conclusions

The line-shape and relaxation times for these poly(propylene glycol)/urethane systems are found to be strongly dependent upon the molecular weight between cross-links and on temperature. The combined line-shape and relaxation time motional information even with the limited state of theory and modeling lead us to several interesting conclusions regarding the motion of the cross-link point in these systems. The observed decrease in linewidth with increasing temperature or increasing M_c nicely reflects the increased mobility of the cross-link point. The cross-link point even with M_c 3K well above the T_g of the segments is not tumbling isotropically although the higher M_c makes the motion more nearly isotropic. For the M_c 1K sample studied in detail, the activation energy for the reorientation of the cross-link determined from line-shape analysis has two regimes, suggesting a transition temperature at which the amplitude of reorientation increases. The frequency of reorientation of the cross-link point in these networks is, depending upon M_c, a factor of 3–5 slower than the motion of the carbon segments of the connecting chains.

The correlation times and motional parameters in this work undoubtedly reflect some "anchoring" effect of the bulky cross-link agent on the poly(propylene glycol). Synthetic efforts are underway to prepare simpler network systems free of the bulky cross-link, which will have dynamics more simply comparable to microscopic theories of rubber elasticity.

Performing measurements of this type on stretched samples will result in very interesting details regarding the the role of the cross-link point in the properties of elastomeric materials. Experiments at a series of Larmor frequencies and some modification of theory will be necessary to fully exploit the cross-link dynamics information contained in the effect.

Acknowledgment. We are grateful to Professor H. W. Spiess for discussions leading to clarification of the phasing artifact and further interpretation of the data. We are also grateful to Professors Alan Jones and Paul Inglefield for supplying the diffusion model and jump model programs and for several beneficial conversations on line-shape analysis. We are grateful to Dr. Hans Hespe, Mobay Chemical, Pittsburgh, PA, for the gift of the cross-linking agent Desmodur RF. This work was supported in part by grants from the Office of Naval Research and by the Materials Research Laboratory NSF Grant to the University of Massachusetts.

References and Notes

(1) O'Gara, J. F.; Jones, A. A.; Hung, C.-C.; Inglefield, P. T. *Macromolecules* **1985**, *18*, 1117.
(2) Connolly, J. J.; Inglefield, P. T.; Jones, A. A. *J. Chem. Phys.* **1987**, *86*, 6602.
(3) Bastide, J.; Picot, C.; Candau, S. *J. Macromol. Sci. Phys.* **1981**, *B19*, 13.
(4) Erman, B.; Monnerie, L. *Macromolecules* **1986**, *19*, 2745.
(5) (a) de la Batie, R. D.; Laupretre, F.; Monnerie, L. *Macromolecules* **1988**, *21*, 2045. (b) *Ibid.* **1988**, *21*, 2052.
(6) Dickinson, L. C.; Morganelli, P.; Chu, C.-W.; Petrovic, Z.; MacKnight, W. J. Chien, J. C. W. *Macromolecules* **1988**, *21*, 338.
(7) Dickinson, L. C.; MacKnight, W. J.; Chien, J. C. W. *J. Polym. Sci., Part C: Polym. Lett.* **1988**, *26*, 191.
(8) Nishi, T. *J. Polym. Sci., Polym. Phys. Ed.* **1974**, *12*, 685.
(9) Muncie, G. C.; Jonas, J.; Rowland, T. J. *J. Polylm. Sci., Polym. Chem.* **1980**, *18*, 1061 and references therein.
(10) Folland, R.; Charlesby, A. *Polymer* **1979**, *20*, 211 and references therein.
(11) Cohen-Addad, J. P.; Domaro, M.; Herz, J. *J. Chem. Phys.* **1982**, *76*, 2744. Cohen-Addad, J. P.; Viallat, A.; Huchot, P. *Macromolecules* **1987**, *20*, 2146.
(12) Gronski, W.; Stadler, R.; Jacobi, M. M. *Macromolecules* **1984**, *17*, 741. See references therein for a number of other orientational order studies.
(13) Deloche, B.; Samulski, E. T. *Macromolecules* **1981**, *14*, 575.
(14) Rance, M.; Byrd, R. A. *J. Magn. Reson.* **1983**, *52*, 221.
(15) Conner, C.; Naito, A.; Takegoshi, K.; McDowell, C. A. *Chem. Phys. Lett.* **1985**, *113*, 123.

(16) Sillescu, H. *J. Chem. Phys.* **1971**, *54*, 2110.
(17) Bloembergen, N.; Purcell, E. M.; Pound, R. V. *Phys. Rev.* **1948**, *73*, 679.
(18) Mehring, M. *High Resolution NMR in Solids*; Springer-Verlag: New York, 1983; 2nd ed.
(19) Spiess, H. W. In *NMR: Basic Princ. Prog.* **1978**, *15*, 55.
(20) Blicharski, J. S. *Z. Naturforsch.* **1972**, *27A*, 1355, 2456.
(21) Howarth, O. *J. Chem. Soc., Faraday Trans. 2* **1979**, *75*, 863.
(22) Dickinson, L. C., in progress.
(23) Jarry, J. P.; Erman, B.; Monnerie, L. *Macromolecules* **1988**, *19*, 2750.
(24) Oeser, R.; Ewen, B.; Richter, D.; Farago, B. *Phys. Rev. Lett.* **1988**, *60*, 1041.
(25) Wemmer, D. E. Ph.D. Thesis, University of California at Berkeley, 1978.

Registry No. (propylene glycol)(tris(4-isocyanatophenyl)-thiophosphate) (copolymer), 124687-67-8.

Mechanistic Reaction Kinetics of 4,4′-Diaminodiphenyl Sulfone Cured Tetraglycidyl-4,4′-diaminodiphenylmethane Epoxy Resins†

Leroy Chiao

Lawrence Livermore National Laboratory, Chemistry and Materials Science Department, Livermore, California 94550. *Received June 12, 1989; Revised Manuscript Received August 28, 1989*

ABSTRACT: A mechanistic kinetic model of 4,4′-diaminodiphenyl sulfone cured tetraglycidyl-4,4′-diaminodiphenylmethane epoxides is developed, which accurately describes experimental data published in the literature. The model is based on an accepted reaction mechanism, which consists of three main reactions. Other efforts to quantitatively model epoxy cure generally focus on empirical rate laws, which apply only to the conditions to which they are fit. It is demonstrated that a mechanistic approach results in a model that can predict the effects of moderate variations in the resin formulation, without being cumbersome or impractical. Moreover, the mechanistic model, unlike the empirical ones, is capable of estimating the relative amounts of linkages formed during the cure reactions. These data offer some insight into the cured resin morphology, which determines the mechanical properties of the material.

Introduction

Epoxy resins based on 4,4′-diaminodiphenyl sulfone (DDS) cured tetraglycidyl-4,4′-diaminodiphenylmethane (TGDDM) are currently the most commonly used matrix material for advanced fiber composites. It is desirable to understand the reaction kinetics of these epoxies for processing purposes. In this work, mechanistic rate expressions are written for the main reactions according to an accepted reaction mechanism. The resulting kinetic model is compared to published literature data.

There have been a number of experimental studies on the cure of DDS/TGDDM resins published in the literature. Most of these efforts utilize differential scanning calorimetry (DSC) to estimate overall degree of cure as the reactions proceed.[1-4] The disadvantage of this method is that the contributions of the individual reactions are not elucidated. Moreover, the method assumes implicitly that the reaction enthalpies of the important reactions are similar, which may not be true.[5] Recently, Morgan and Mones[6] performed an extensive Fourier-transform infrared (FTIR) spectroscopy analysis of DDS/TGDDM epoxies, which yielded cure data on the individual species involved.

To date, virtually all thermoset polymer kinetic models that appear in the literature are based on empirical rate laws.[1-4,7,8] These empirical rate laws have been used successfully in modeling studies.[9-15] However, there are advantages to using mechanistic kinetic models: (1) Unlike empirical models, moderate changes in the resin formulation that do not change the reaction mechanism would not require recharacterization, because the contributions of the individual chemical components are described. (2) Extrapolated behavior of the resin system outside of the envelope from which the kinetic parameters were fitted is more predictable, since the temperature dependencies of the individual reactions involved are known. With empirical models, the resin behavior is only predictable over the temperature range used to characterize it. (3) Unlike empirical models, which can only estimate relative degree of cure, mechanistic models account for individual chemical species. Thus, they offer some insight into the cured resin morphology, which determines the material mechanical properties.[6,16]

Model Development

The structures of the TGDDM and DDS monomers are shown in Figure 1. It is generally agreed that there are three main reactions that occur for amine-cured epoxies:[3,6,17,18] Reactions 1 and 2 are the primary and

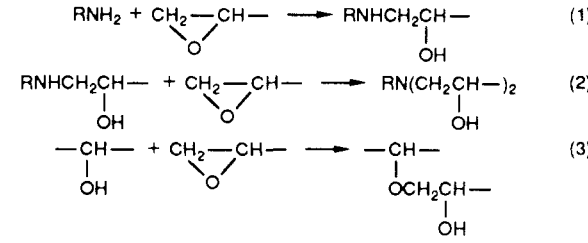

† Work performed under the auspices of the U.S Department of Energy by the Lawrence Livermore National Laboratory under Contract W-7405-ENG-48.

0024-9297/90/2223-1286$02.50/0